scientific reports

Check for updates

OPEN

Exosomes derived from hypoxic mesenchymal stem cell ameliorate premature ovarian insufficiency by reducing mitochondrial oxidative stress

Shanshan Zhang[1,4], Xinfeng Zou[2,4], Xiaona Feng[1], Shuai Shi[3], Yanyun Zheng[1], Qun Li[1] & Yanqun Wu[1]✉

Cyclophosphamide (CTX) exposure causes premature ovarian insufficiency (POI). The therapeutic potential of exosomes derived from human umbilical cord mesenchymal stem cells (hucMSCs) is not fully understood, especially regarding whether hypoxic preconditioning enhances their efficacy in POI. In this study, exosomes were isolated and identified from hucMSCs (hucMSCs-Exos) under hypoxic (HExos) and normoxic (NExos) conditions. Cyclophosphamide (CTX) was used to develop the POI rat model, and NExos or HExos was injected into the tail vein to investigate its therapeutic effect on POI. In addition, CTX-treated KGN cell lines were used to investigate the effects of NExos and HExos on cell proliferation, apoptosis, oxidative stress and mitochondrial membrane potential.The results indicated that hucMSCs-Exos transplantation substantially improved body weight, ovarian weight coefficient, estrous cycles, ovarian morphology, ovulation count, and sex hormone levels in POI rats. Further, HExos showed a higher level of therapeutic efficiency than NExos. In vitro experiments demonstrated that NExos and HExos may be phagocytosed by KGN cell line, decrease cell apoptosis, and enhance cell growth. After NExos or HExos transplantation, the reactive oxygen species level was reduced, mitochondrial membrane potential enhanced, and the levels of mitochondrial oxidative stress-associated factors returned to their basal level. Notably, the improvement of oxidative stress by NExos or HExos was blocked by the SIRT3 selective inhibitor 3-TYP. In conclusion, hypoxia-induced hucMSCs-Exos protected the ovarian reserve against CXT-induced ovarian damage by rectifying mitochondrial malfunction *via* the SIRT3/PGC1-α pathway, establishing a solid basis for developing specific ovarian protection therapies.

Keywords Mesenchymal stem cells, Premature ovarian insufficiency, Exosomes, Reactive oxygen species, Hypoxic

Abbreviations

CTX	Cyclophosphamide
POI	Premature ovarian insufficiency
hucMSCs	Human umbilical cord mesenchymal stem cells
NExos	HucMSCs under normoxia
HExos	HucMSCs under hypoxia
GCs	Granulosa cells
FSH	Follicle-stimulating hormone
E_2	Estradiol
OS	Oxidative stress
TEM	Transmission electron microscopy
NTA	Nanoparticle tracking analysis

[1]School of Life sciences, Jining Medical University, Rizhao City, Shandong, China. [2]Shandong Xinchao Biotechnology Co., Ltd., Rizhao City, Shandong, China. [3]IVF center, Jinhua People's Hospital, Jinhua City, Zhejiang, China. [4]Shanshan Zhang and Xinfeng Zou contributed equally to this work. ✉email: yqwu@mail.jnmc.edu.cn

BW	Body weight
IVF	In vitro fertilization
ROS	Reactive oxygen species
MMP	Mitochondrial membrane potential

Premature ovarian insufficiency (POI) is a gynecological and endocrine condition characterized by impaired ovarian function in women under the age of 40 years[1]. The primary symptoms are amenorrhea, increased follicle-stimulating hormone (FSH), and lowered estradiol (E_2) levels. The known etiology of POI involves genetics, autoimmune, iatrogenic, metabolic abnormalities, and environmental pollutants[2]. Research indicates that more than 40% of women might suffer POI after chemotherapy, raising significant concerns about the possibility of ovarian damage due to chemotherapeutic agents[3,4]. Therefore, it is necessary to investigate chemotherapy-mediated POI and to formulate safer and more potent approaches for its management.

Mesenchymal stem cells (MSCs) can reduce ovarian senescence and failure. Human umbilical cord MSCs (hucMSCs) are widely used due to their easy isolation process, low or negligible immunogenic response, and high proliferation potential[5,6]. The primary function of hucMSCs is the secretion of various bioactive molecules, and exosomes are an essential component of these paracrine secretions[7]. Exosomes are a subtype of extracellular vesicles, typically between 30 and 200 nm, known to transport a range of biological compounds such as cytokines, mRNA, miRNA, and proteins[8,9]. Through the binding of surface ligands to target cells and the delivery of their internal contents, exosomes regulate a variety of biological processes, often reflecting the functional properties of their source cells[10,11]. Several studies have revealed that hucMSCs-Exos can enhance the ovarian reserves[11], hormone levels[7], oxidative stress (OS) responses[7], and immunological reactions[12] of POI rats by delivering bioactive factors and functional RNAs.

The concentration of oxygen has been recognized to be vitally important in the process of proliferation, differentiation and self-renewal of MSCs[13]. However, during in vitro culture conditions, MSCs are usually exposed to normoxia (21% O_2) which is very different to the oxygen concentrations found in the body under natural physiological conditions. In fact, a large proportion of MSCs exist in a hypoxic environment (2–8% O_2 or even lower) in the body[14,15]. Hypoxic conditions may enhance the stemness and paracrine secretion of MSCs, accelerate the synthesis of exosomes[15,16], and increase their biological roles and activities, thereby increasing their therapeutic efficiency against diseases[15,17].

However, whether hypoxia improves the therapeutic efficacy of hucMSC-Exos in POI remains unclear. Thus, this study explored the biological effects of hucMSC-Exos under hypoxia on POI. This study also investigated the impact of hucMSCs under normoxia (NExos) and hypoxia (HExos) on CTX-induced granulosa cells (GCs) propagation and apoptosis. It was depicted that HExos may inhibit CTX-induced POI by modulating mitochondrial OS.

Results

hucMSCs and hucMSC-Exos characterization

Surface markers of hucMSCs were examined to confirm that they are a type of MSCs. Their morphological features (4th passage) were observed under a phase-contrast microscope. There was no difference in the morphology of hucMSCs cultured under 1% hypoxic and 21% normoxic conditions (Fig. 1A). Both showed swirling and fibroblast-like morphology. Cell count and CCK8 results showed that hucMSCs cultured under normoxia or hypoxia had no difference in cell number and cell viability (Fig. 1B-C). Similarly, mesenchymal markers such as CD90, CD73, and CD105 showed positive expression for hucMSCs, while hematopoietic markers like CD45, CD34, and HLA- DR displayed negative expression in both conditions (Fig. 1D).

After incubating hucMSCs under normoxia and hypoxia for 48 h, supernatant media were collected to extract exosomes. Hypoxia-Exos and Normoxia-Exos showed similar round vesicles as examined through transmission electron microscopy (TEM) (Fig. 2A). Exosome surface markers, including CD81 and synthenin, were observed using WB analysis (Fig. 2B). Nanoparticle tracking analysis (NTA) revealed that Hypoxia-Exos and Normoxia-Exos had similar size distributions (40 to 150 nm in diameter, Fig. 2C-D). In contrast, Hypoxia-Exos had a considerably higher concentration (Fig. 2E), indicating remarkable exosome secretion by hucMSCs under hypoxic conditions. We examined HIF-1α expression and showed that upregulated HIF-1α expression was detected in HExos compared to NExos (Fig. 2F).

HExos improved the function of the ovary more forcefully than NExos in POI rats

The rats were weighed after a week of CTX administration. The body weight (BW) of POI rats decreased substantially after 2 weeks (Fig. 3A). Relative to the POI group, the NExos group had substantially higher BW, which increased this favorable effect in the HExos group. In contrast to the POI group, the weight of the ovary and the organ coefficient ratio of the ovaries in the NExos and HExos groups remarkably increased, and it was more significant in the HExos group (Fig. 3B-D).

The estrous cycle of POI rats remained irregular throughout the experiment, while HExos and NExos rats recovered gradually after hucMSC-Exos transplantation (Fig. 3E -F). In contrast to the control group, FSH levels were considerably increased, and E_2 levels substantially lowered in the POI group, which normalized after treatment with NExos and Hexos (Fig. 3G-I). These findings indicated that NExos and HExos therapy improved ovarian function in POI rats and that HExos was more effective than NExos.

The number and development of follicles in the ovaries were examined at all stages *via* H&E staining (Fig. 4A-B). The control group showed mature primordial, primary, secondary, and antral follicles. In contrast, the POI rat model showed atrophied ovaries with decreasing follicles at each stage. The number of follicles was substantially lower in the POI group than in the NExos group, while the number of primary, secondary, and

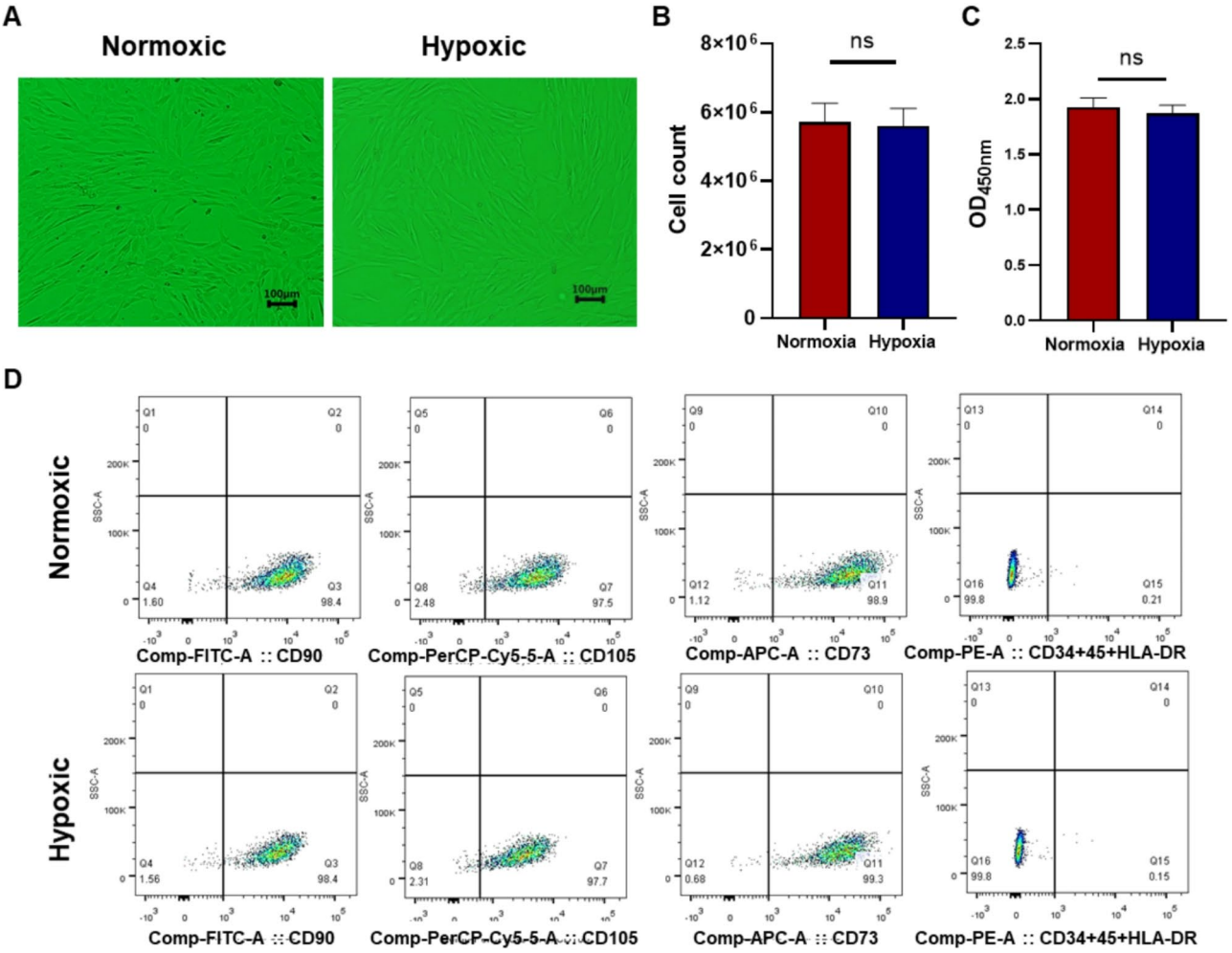

Fig. 1. Characterizations of hucMSCs under normoxic/hypoxic culture conditions. (**A**) Representative images of morphological features of hucMSCs under the light microscope (Scale bar = 100 μm). (**B**) The number of hucMSCs cultured under normoxic and hypoxic conditions. (**C**) Cell viability was determined by CCK-8 assay. (**D**) Flow cytometric analysis of hucMSCs.

antral follicles was considerably higher in the HExos group. These results suggest that HExos revealed a better therapeutic effect on follicle recovery.

Superovulation results demonstrated a significant decline in the follicle number in the POI group, which could be restored by transplantation of hucMSC-Exos (Fig. 4C-D). The number of eggs in the HExos group was more elevated than in the NExos group. After that, the In vitro fertilization (IVF) ability of oocytes from each group was evaluated. The rates of fertilized eggs and blastocysts in the POI group were reduced after IVF with the donor sperm, which was later restored by NExos or HExos transplantation, where HExos depicted better recovery than NExos (Fig. 4E-F). Altogether, these results suggest that HExos possesses better protective and regenerative effects for follicle damage and development in vivo relative to the NExos group.

NExos and HExos enhanced KGN cell proliferation and reduced CTX-induced apoptosis in KGN cells

The dysfunction of ovarian GCs directly affects the POI. Studies showed that CTX substantially induced mouse ovarian atrophy and inhibition of GCs proliferation[18,19]. To examine the effect of HExos and NExos on internalized GCs, the exosomes were labeled with Dio fluorescent dye and co-cultured with KGN cells. The green fluorescence in exosomes was detected in the perinuclear region of GCs, indicating that Dio-labeled NExos and HExos can penetrate the cytoplasm of GCs (Fig. 5A). This phenomenon of phagocytosis well supports the potential functional impact of NExos and HExos on GCs.

To further observe the protective role of NExos and HExos on GCs, a POI cell model was developed based on the co-culture of KGN cells with 1 mg/mL CTX to trigger apoptosis and evaluated the effects of NExos and HExos on GCs survival and apoptosis. It was also observed that NExos and HExos considerably promoted GCs proliferation and reduced the ratio of early apoptotic GCs induced by CTX (Fig. 5B-C). Cell apoptosis was controlled by the significant activators *caspase-3* and *9*. The study also measured *caspase-3* and *9* expression in the ovaries of rats. The findings showed that the fold expression of *caspase-3* and *9* was intensely elevated in the

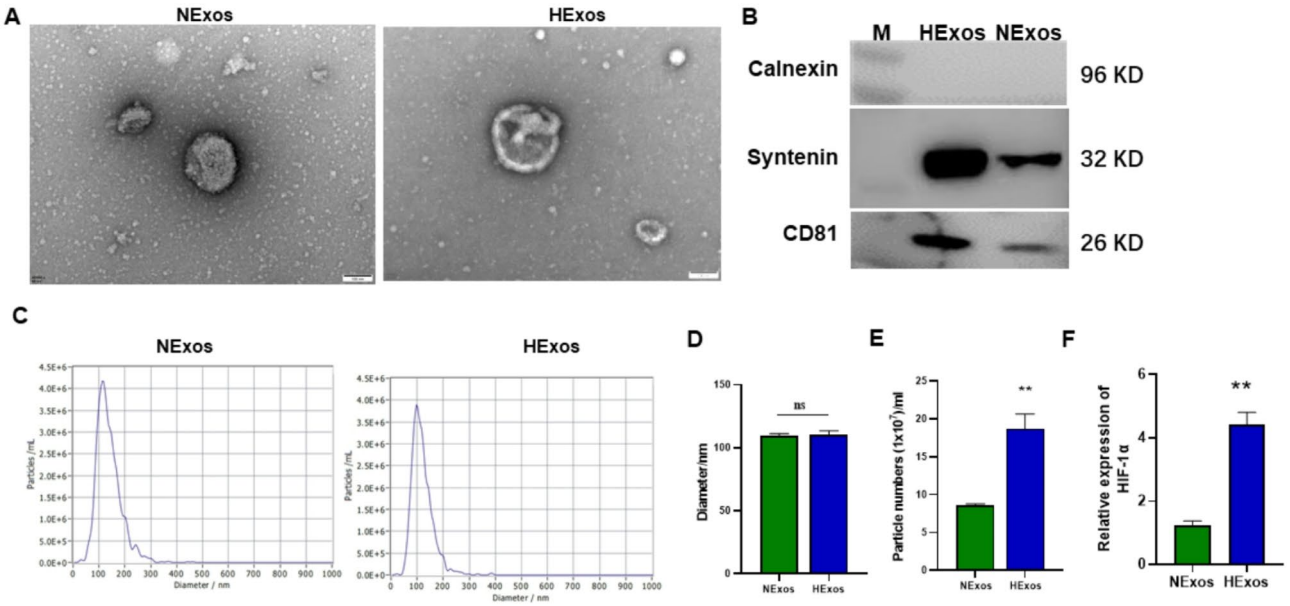

Fig. 2. Characterizations of hucMSC-NExos and hucMSC-HExos. (**A**) TEM image of NExos and HExos (Scale bar = 100 nm). (**B**) Detection of the protein levels of hucMSC-Exos markers in NExos and HExos (negative for Calnexin and positive for CD81 and Syntenin) *via* WB analysis. (**C**–**E**) Evaluation of size and concentration of NExos and HExos *via* NTA. (**F**) The mRNA level of HIF1α in NExos and HExos was detected by qPCR. Data was statistically examined *via* Student's t-test and illustrated as mean ± SEM (** $p < 0.01$).

POI group relative to the control; their expressions were returned to the normal state in the NExos and HExos groups (Fig. 5D-E). We also assessed the protein expression levels of key pro-apoptotic factors in the ovaries of rats in each group. As shown in Fig. 5F-G, the expression levels of pro-apoptotic proteins (including cleaved caspase3, bax, and p53) in the NExos and HExos groups were significantly lower than those in the POI group, and the expression levels of various pro-apoptotic proteins in the HExos group were lower than those in the NExos group.

HExos inhibited CTX-induced mitochondrial reactive oxygen species (ROS) than NExos via SIRT3/PGC-1α signaling pathway

CTX has been reported to induce high levels of oxidative stress and apoptosis in human GCs[20]. The level of cellular ROS was measured quantitatively using a DCFH-DA fluorescent probe. The levels of ROS in CTX-damaged KGN were remarkably decreased after the treatment of NExos and HExos (Fig. 6A). However, the levels of ROS produced by the HExos treatment were substantially lower than those generated by the NExos treatment.

Mitochondria are the primary source of ROS synthesis and are more susceptible to OS. The effect of NExos and HExos on CTX-induced mitochondrial membrane potential (MMP) in KGN cells was determined using the JC-1 probe. JC-1 penetrates mitochondria in the presence of depolarized MMP and reversibly changes color as the MMP changes. As shown in Fig. 6B, CTX-exposed cells emitted a significant green fluorescence, indicating a depolarized mitochondrial membrane. Simultaneously, pretreatment with NExos and HExos had an inhibitory effect on CTX-induced alterations of MMP, marked by a decrease in green fluorescence along with restoring red fluorescence. This indicates that NExos and HExos protect against the collapse of mitochondrial membrane potential in GCs by CTX.

RT-qPCR results depicted that the levels of *SOD2*, *SIRT3*, *PGC1-a*, and *TFAM*, the major regulators of mitochondrial function and ROS stress response, were substantially lowered in the ovaries of POI rats. Simultaneously, NExos or HExos treatment considerably increased their expressions. These positive effects were more pronounced after HExos treatment (Fig. 6C-F).

To further prove that NExos and HExos regulate mitochondrial function and oxidative stress through the SIRT3/PGC-1α signaling pathway, we used SIRT3 inhibitors (3-TYP) to knock down SIRT3/PGC-1α under NExos and HExos treatment. RT-qPCR results showed that 3-TYP could significantly inhibit the expression of SIRT3, SOD2, PGC1a and TFAM (Fig. 7A). DCFH-DA and JC-1 fluorescent probes were used to quantitatively evaluate intracellular ROS and MMP levels, respectively, to demonstrate the relationship of SIRT3/PGC-1α signaling pathway in the regulation of mitochondrial function and oxidative stress by NExos and HExos. The results showed that NExos and HExos could reduce the ROS fluorescence intensity of KGN cells induced by CTX. After addition of SIRT3 inhibitor 3-TYP, the peak of cell population shifted to the right and the average fluorescence intensity increased significantly (Fig. 7B). At the same time, the green fluorescence of JC-1 probe was significantly decreased in NExos and HExos treated cells, while the green fluorescence intensity of cells was significantly increased after the addition of 3-TYP, indicating mitochondrial depolarization (Fig. 7C).These

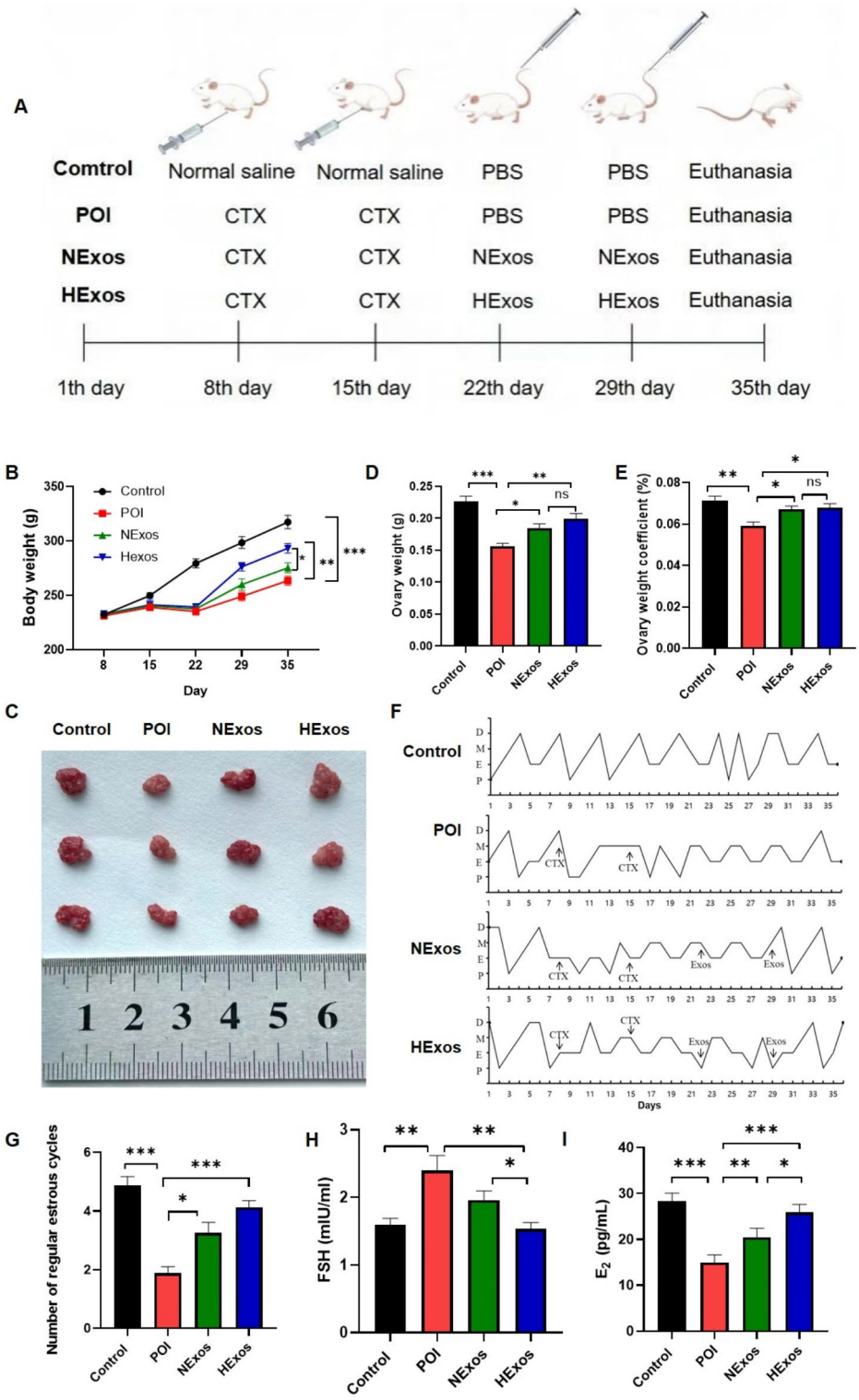

Fig. 3. HExos improves body weight and ovarian function more effectively than NExos in POI rats. (**A**) Treatment procedure of POI using hucMSCs. (**B**) Changes in the weight of all groups of rats. (**C**) Ovary size of rats in different groups. (**D**) Ovary weight changes in all groups of rats. (**E**) Ovary weight coefficient of all groups of rats. (**F**) Clear cycle curves of rats in different groups. (**G**) Each group of rats contained complete clearance cycles. Serum FSH (**H**) and E_2 (**I**) levels of rats in different groups. Three distinct experiments were evaluated *via* Student's t-test, with error bars illustrated as means ± SEM (*$p < 0.05$, **$p < 0.01$, ***$p < 0.001$).

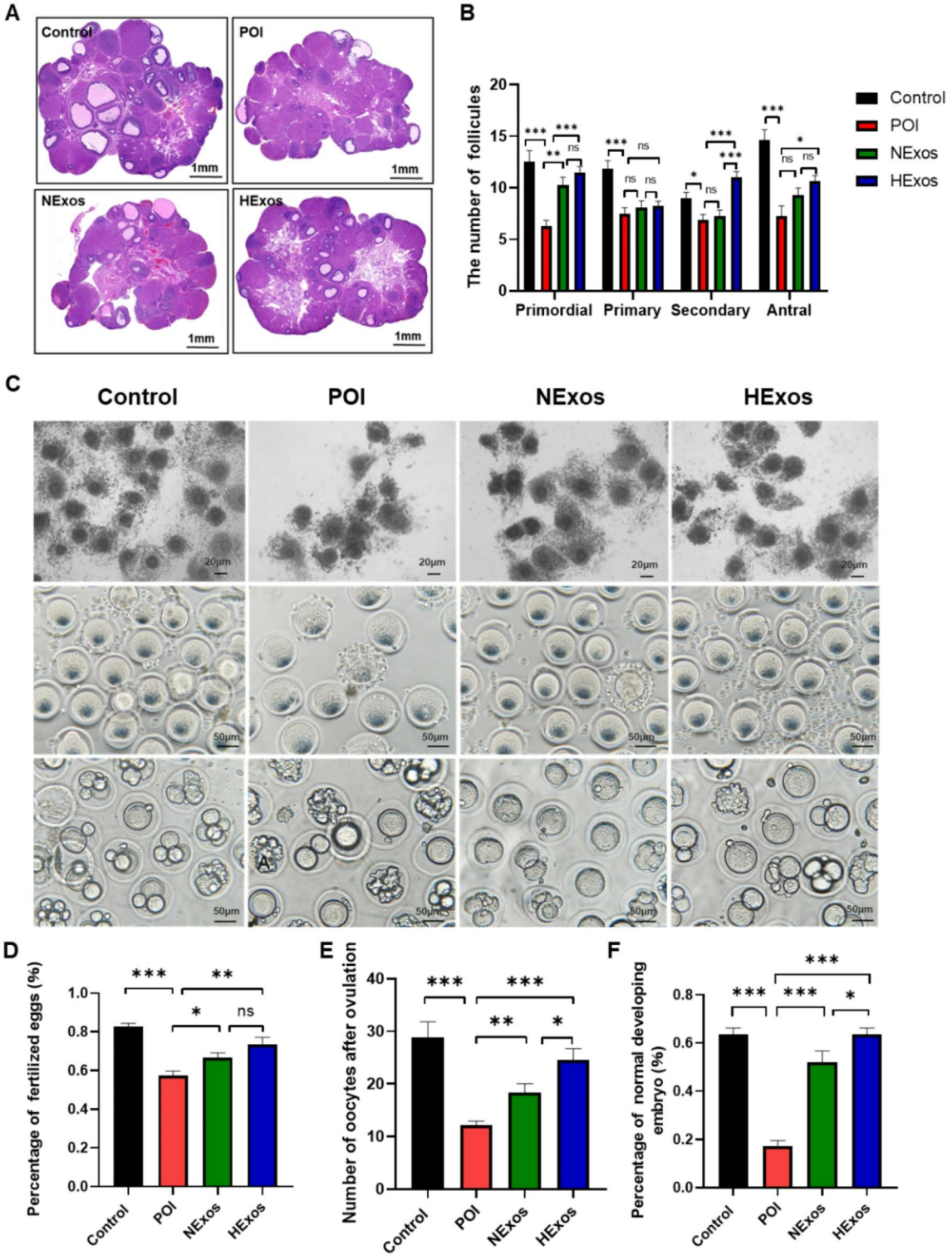

Fig. 4. HExos improved ovarian morphology and follicular development than NExos in POI rats. (**A**) Histopathological images of ovarian tissue sections *via* H&E staining (Scale bar = 1 mm). (**B**) Quantification of the ovarian follicle at different stages of development. (**C**) Bright-field images of in vitro embryo development. From top to bottom and left to right: cumulus-oocyte complexes, fertilized eggs with the second polar body, normally developing embryo. (**D**) Number of oocytes per group after superovulation. After IVF, the percentage of fertilization with two cells (**E**) and a normal developing embryo (**F**). Three distinct experiments were evaluated *via* Student's t-test, with error bars illustrated as means ± SEM (*$p < 0.05$, **$p < 0.01$, ***$p < 0.001$).

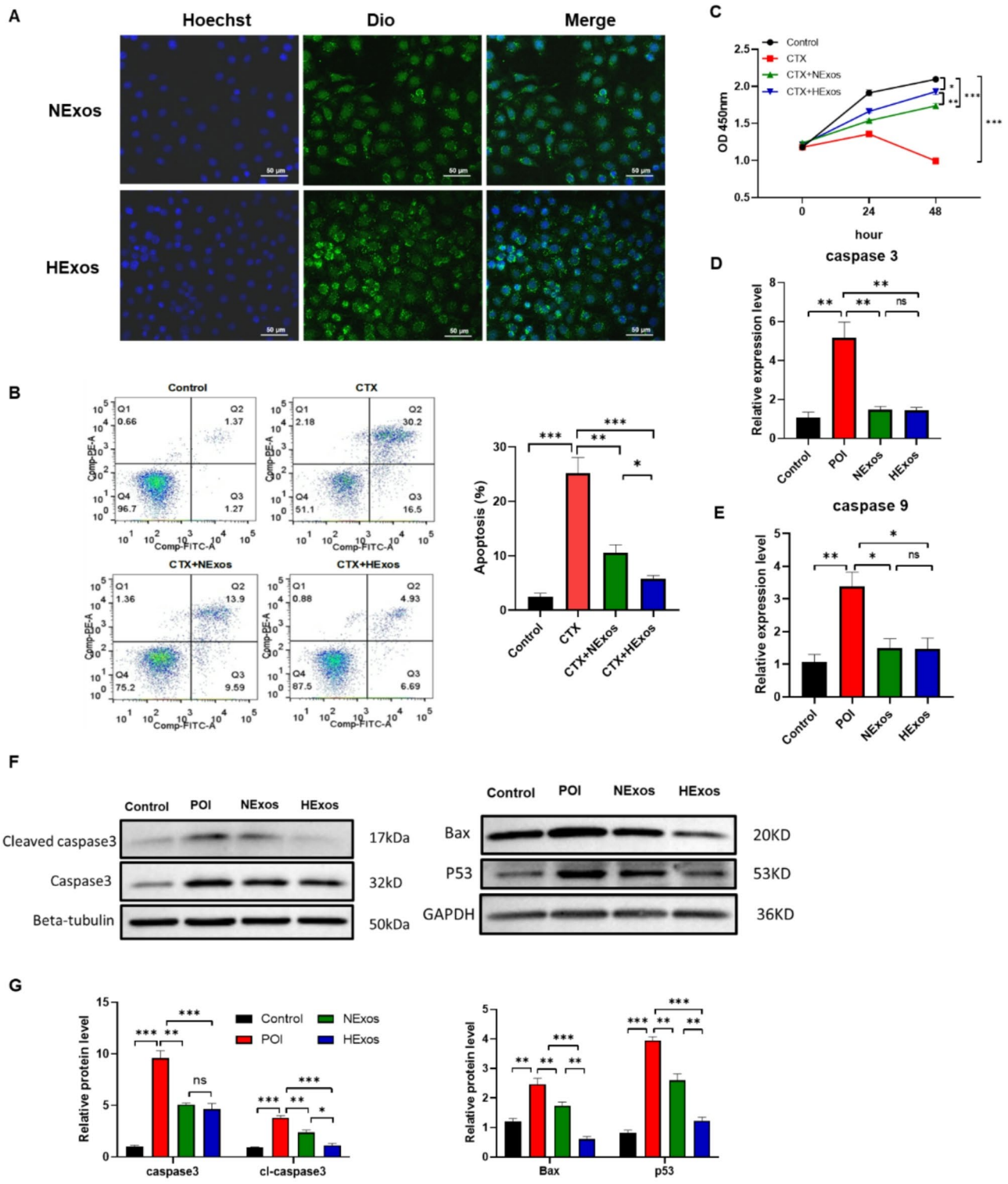

Fig. 5. NExos and HExos accelerated KGN cell propagation and attenuated CTX-induced KGN cell apoptosis. (**A**) Uptake of the green fluorescence dye Dio labeled NExso and HExos into KGN cells (Scale bar = 50 μm). (**B**) Detection of cell apoptosis of different groups by flow cytometry. (**C**) Detection of cell proliferation curves by CCK-8 assay. (**D**) Detection of mRNA levels of *caspase 3* in the ovary of different rat groups. (**E**) Detection of mRNA levels of *caspase 9* in the ovary of different rat groups. (**F**) Apoptosis protein expression analysis in the ovary of different rat groups. (**G**) The histogram summarizes the protein expression levels. Three distinct experiments were evaluated *via* Student's t-test, with error bars illustrated as means ± SEM (*$p < 0.05$, **$p < 0.01$, ***$p < 0.001$).

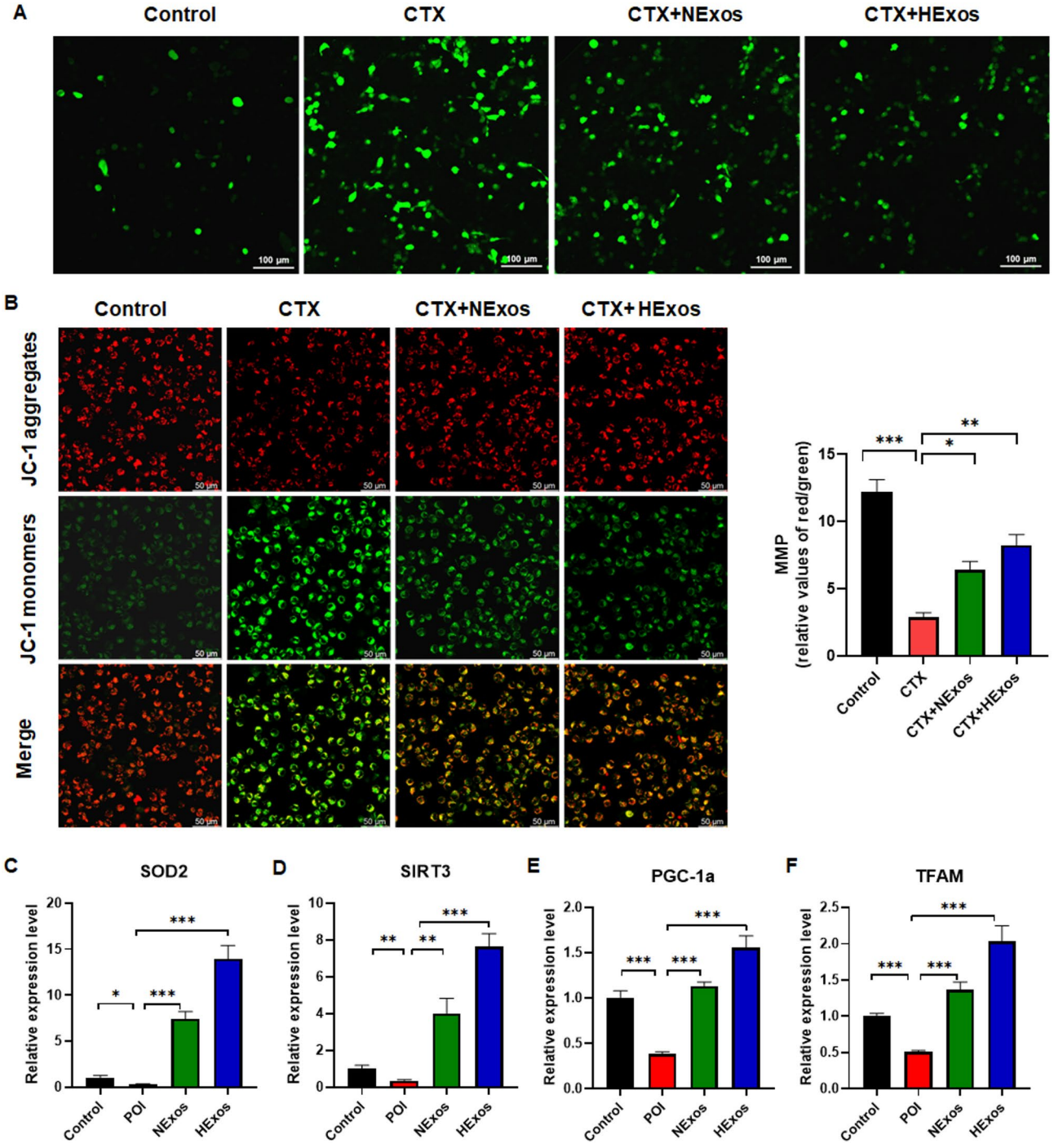

Fig. 6. HExos inhibited CTX-induced oxidative stress than NExos in KGN cells. (**A**) Detection of ROS levels in different groups by immunofluorescence staining (Scale bar = 50 μm). (**B**) Laser confocal microscopic images of cells treated with a JC-1 fluorescent probe and JC-1 aggregates (red) and JC-1 monomers (green). Detection of mRNA levels of *SOD2* (**C**), *SIRT3* (**D**), *PGC1-a* (**E**), and *TFAM* (**F**) in the ovary of rats in different groups. Three distinct experiments were evaluated *via* Student's t-test, with error bars illustrated as means ± SEM (*$p < 0.05$, **$p < 0.01$, ***$p < 0.001$).

results suggest that NExos and HExos regulate mitochondrial function and oxidative stress via the SIRT3/PGC-1α signaling pathway.

Discussion

The prevalence of POF in females is 1%[21], and CTX treatment is one of the main reasons for this condition[22]. Therefore, the restoration of ovarian function and the treatment of degenerative ovarian changes are crucial

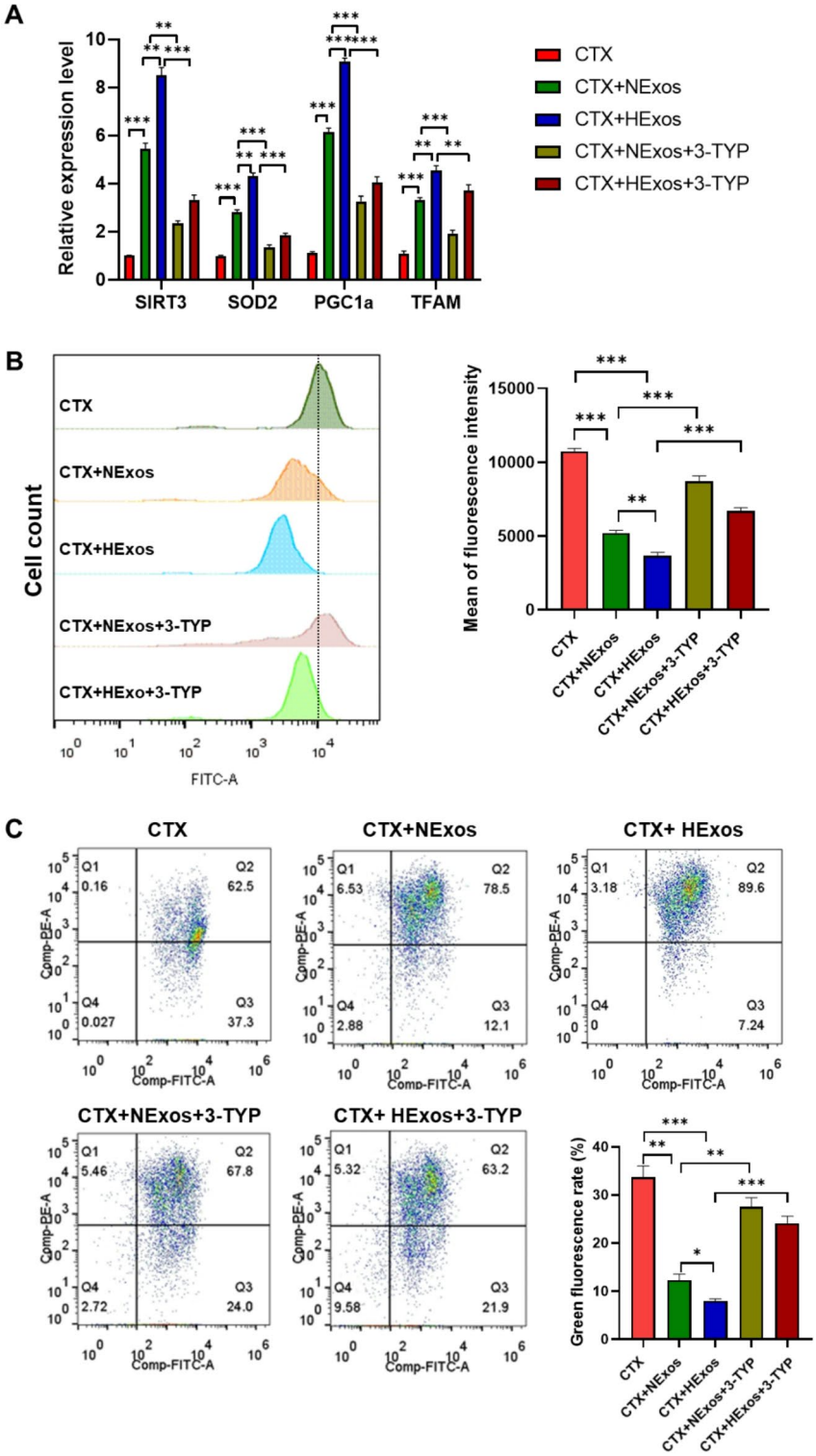

Fig. 7. NExos and HExos regulate mitochondrial function and oxidative stress through the SIRT3/PGC-1α signaling pathway. (**A**) The expression of SIRT3, SOD2, PGC1a and TFAM in KGN cells was detected by RT-qPCR. (**B**) The ROS levels were detected by flow cytometry. (**C**) Flow cytometry analysis quantified changes in MMP across experimental groups. Three distinct experiments were evaluated via Student's t-test, with error bars illustrated as means ± SEM (*$p < 0.05$, **$p < 0.01$, ***$p < 0.001$).

for maintaining female fertility health[23]. Cell therapy, such as human MSCs, is a novel approach to preserving ovarian function and addressing female infertility[24]. After childbirth, the umbilical cord is regarded as a waste bioproduct; however, huc-MSC shows distinct benefits over MSCs isolated from other sources, such as bone marrow or adipose tissue. They show high proliferation potential and enhanced pluripotency[25], thereby being more appropriately used for cell therapy. However, their application is restricted by challenges such as immunogenicity, malignant transformation, embolism, inadequate cell engraftment, and post-transplantation survival[26]. Importantly, exosomes are distinguished by their lack of expression of major histocompatibility complex I or II, which addresses all cell therapy's drawbacks[27].

Exosomes responded more efficiently to various stimuli, including inflammation and hypoxic environments[28,29]. Recent research has revealed that exosomes are crucial in protecting ovarian function, providing a new direction for preventing and treating ovarian diseases[11,30,31]. Conversely, it is not well known whether hypoxia-pretreated hucMSCs-Exos show enhanced biological effects on POI. To investigate this effect, hucMSCs were cultured under 21% normoxic and 1% hypoxic environments, and their exosomes were extracted and characterized. In the findings, no morphological differences in size and shape were detected between the HExos and NExos. However, studies have also shown that hypoxic conditions can promote exosome secretion from hucMSCs.

In line with previous studies, exosomes obtained from hucMSCs (hucMSC-Exos) under normoxic conditions showed therapeutic efficacy in the in vivo treatment of POI. This study identified the role of hucMSC-Exos in hypoxic conditions, revealing that HExos had enhanced therapeutic efficacy in POI relative to normoxic conditions, and its mechanism of action may be related to the induction of hypoxia. The findings represent that hypoxia priming may be an effective alternative for improving the therapeutic efficacy of hucMSC-Exos in POI.

The main mechanism of CTX-induced POI may involve directly targeting oocytes or indirectly inducing oocyte apoptosis *via* damage to GCs[4]. Moreover, GCs are essential for assessing the fate of follicles. The effects of HExos on GCs were examined further to investigate the underlying mechanisms. Mitochondria, which serve as the power source of cells, play a considerable role in various physiological functions. It is suggested that their dysfunction is one of the leading factors in the development of POI[32,33]. Growing evidence demonstrates the significance of ROS in inducing mitochondrial dysfunction. Excess ROS after the progression of POI causes oxidative damage to nucleic acids, proteins, and lipids, leading to cell death[34]. ROS production can enhance ovarian granulosa cell death and follicular atresia, with increased ROS levels serving as a crucial factor in cyclophosphamide-induced POI[35,36]. This study found that HExos markedly reduced cyclophosphamide-induced oxidative stress, mitochondrial membrane potential impairment, and reduced apoptosis in ovarian granulosa cells.

This study emphasizes the potential of hypoxic-induced hucMSCs-Exos to impede chemotherapy-mediated ovarian toxicity, thereby establishing a solid basis for developing targeted ovarian protection strategies. Further studies may investigate the interaction between exosomes and ovarian cells to clarify their specific regulatory functions in maintaining ovarian efficiency.

This study also has limitations and potential future directions. Despite the positive indications from the current findings, additional, comprehensive evaluation and validation are necessary before clinical use. Future research could examine the biological features and operational mechanisms of exosomes to identify more precise and effective treatments, thereby expanding the range of options for managing chemotherapy-mediated POI.

Further, the ethical implications of using human-derived cells and standardizing exosome purification procedures require extra consideration. Further research is necessary to comprehend the dosage, route of administration, and potential effects of exosomes on the human body in clinical settings.

Methods

Animals

In this study, SD female rats (8 weeks) were obtained from Jinan Pengyue Laboratory Animal Breeding Co. LTD (Jinan, China) and kept in the barrier system of the animal experiment center located at Jining Medical University. These animals were housed in a nonpathogenic environment with specific conditions: 12 h light/dark cycle (lights on at 7:00 a.m) and 22 ± 2 °C. All experiments involving animals were conducted in accordance with protocols approved by the Animal Welfare & Ethics Committee of Jining Medical University (JNMC-2022-DW-167), mice were euthanized using carbon dioxide (CO_2) inhalation before used for tissue collection. All procedures followed ethical guidelines for animal experiments.

Development of POI rat model and hUMSC-Exos treatment

As depicted in Fig. 3A, the experiment comprised four groups: control ($n = 8$), POI ($n = 8$), POI + Hypoxia-Exos (HExos, $n = 8$), and POI + Normoxia-Exos (NExos, $n = 8$) groups. To develop the POI model, rats were injected CTX (120 mg/kg) intraperitoneally for two weeks (once a week), whereas the control group was administered with an equal volume of normal saline.

Once the POI model was developed, 200 µL of HExos or NExos (1×10^9 cells) was transplanted into each ovary for two weeks (once a week) in the POI + HExos and the POI + NExos groups. Similarly, rats in the POI group were administered an equal volume of PBS. Vaginal smears were collected daily at 8 a.m. to assess the estrous cycle.

Isolation and identification of hucMSCs

Ethical approval (AJYX-2023-XB-01) was obtained from the Augie Medical Ethics Committee of Rizhao City to collect the umbilical cord tissue, and was conducted in accordance with the principles of the Declaration of Helsinki. All patients signed written informed consent for study participation. HucMSCs were harvested from this tissue using the tissue block adhesion method[37] and then cultured in Dulbecco's Modified Eagle's Medium

(DMEM) (Gibco, USA) with 10% fetal bovine serum (FBS) (Gibco, USA). Under 1% hypoxic and 21% normoxic conditions, 80–90% confluent hucMSCs (at 4th passage) were grown without serum for 48 h.

Isolated cells were characterized as described previously[30]. Their morphology was examined under a light microscope and confirmed using their specific markers (positive expression for CD34, CD90, CD73, CD105, negative expression for CD45, and HLA-DR) *via* flow cytometry (FC). Fluorescence signals were sorted *via* a flow cytometer (BD Biosciences, USA) and quantified by FlowJo software (Becton Dickinson).

Isolation and characterization of hucMSCs-Exos

For hucMSCs-Exos isolation, the same method was used as mentioned previously[30]. Cells were filtered by spinning the exhausted medium of treated hucMSCs (at 4th passage) for 10 min at 300 × g and 4 °C. To isolate exosomes, the supernatant was spun at 4 °C for 10 min at 2,000 g, followed by 30 min at 10,000 g and 70 min at 100,000 g. The precipitate was rinsed with phosphate-buffered saline (PBS; Servicebio, China) and spun for 70 min at 100,000 g, 4 °C. After that, the precipitate was mixed with chilled PBS and kept at -80 °C.

As previously mentioned[38], the same experiment was performed on hucMSC-Exos identification and characterization. TEM (Talos F200C; Thermo Scientific, US) was used to examine their morphological characteristics. Nanoparticle tracking analysis (NTA) was conducted to quantify their concentration and size distribution. Western blotting (WB) was performed to identify their surface markers, including CD81, TSG101, and syntenin (Biolegend, US).

Western blot analysis

The proteins were extracted with RIPA buffer, separated on polyacrylamide gels using SDS, and then electrotransferred onto membranes made of polyvinylidene fluoride (PVDF). After incubating the membranes for 20 min in NcmBlot blocking buffer (NCM Biotech, China), they were probed overnight at 4 ℃ with primary antibodies specific for the proteins listed below: CD81, TSG101, syntenin, cleaved caspase3, caspase3, Bax, P53, GAPDH, Beta-tubulin (Biolegend, US). Antibody reactivity was detected using an ECL kit (Biosharp, China) and visualized using the ChemiDocTM XRS + system (BIO-RAD, USA).

Hematoxylin and eosin (H&E) staining

The same procedure for H&E staining was followed as outlined previously[39]. Precisely, ovarian tissues were fixed with 4% paraformaldehyde (Beyotime, China), dehydrated, embedded in paraffin, and sectioned to 4 µm. These sections were stained with H&E stains, and the tissue integrity of each section was analyzed under an inverted microscope (Leica DMI1, Germany). Different fields of images were captured, and the number of follicles was quantified.

Hormone analysis

The levels of E_2 and FSH were detected in the serum sample. These measurements were conducted by RIA at the Institute of Beijing North Biotechnology.

Rats superovulation

All rats received an intraperitoneal injection of 7.5 IU of pregnant mare serum gonadotropin (PMSG, Ningbo Second Hormone Factory, China, YMXQ-0001), followed by an intraperitoneal dose of 7.5 IU of human chorionic gonadotropin (HCG, JS0001) 48 h later. The oocytes were harvested 12 to 16 h post-HCG injection.

IVF

Donor sperm were initially collected from male rats and placed in G-IVF media (Vitrolife, Goteborg, Sweden). Media was kept in an oil bath at 37 ℃ with 5% CO_2 for 1 h to facilitate capacitation. Metaphase II oocytes were then added into 250 µL of media containing sperm (2×10^5/mL to 3×10^5/mL) for fertilization. After 6 h, zygotes with fine pronuclei were transferred into fresh G-1 media (Vitrolife) and maintained there for 24 h until the two-cell embryonic stage. G-1 media was used to cultured the fertilized embryos until they reached the blastocyst stage, which lasted for 5 days.

Human granular tumor cell culturing and treatment

KGN cells (Procell CL-0603) were obtained from Wuhan Procell Life Science & Technology Co., Ltd. and were maintained in DMEM/F12 medium enriched with 10% FBS and 1% penicillin/streptomycin (Gibco, USA). These cells were categorized into several distinct groups: (1) control; (2) CTX (1 mg/mL); (3) treatment with CTX (1 mg/mL) and NExos (50 µg/mL) (CYX + NExos); (4) CTX (1 mg/mL) and HExos (50 µg/mL) (HExos) groups; (5) treatment with CTX (1 mg/mL), NExos (50 µg/mL) and 3-TYP (10µM) (CYX + NExos + 3-TYP); (6) treatment with CTX (1 mg/mL), HExos (50 µg/mL) and 3-TYP (10µM) (CYX + HExos + 3-TYP).

Cellular uptake assay

NExos and HExos were resuspended and fluorescently labeled with Dio dye (Biotime, China), which was in line with the provided protocols. KGN cells (4×10^4 cells/well) were cultured on 24-well culture slides and kept overnight. NExos and HExos were labeled with a Dio green fluorescence labeling kit (Beyotime, China) for 10 min, followed by ultrafiltration at 10,000 × g for 20 min using a 10 kDa cutoff membrane to remove unbound dye. Next, the Dio-tagged NExos and HExos were kept with KGN cells for 10 h, after which the cells were counterstained with Hoechst 33,258.

Primer	Sequence
mGAPDH-F	AGGTCGGTGTGAACGGATTTG
mGAPDH-R	TGTAGACCATGTAGTTGAGGTCA
mSP1-F	GCCGCCTTTTCTCAGACTC
mSP1-R	TTGGGTGACTCAATTCTGCTG
mCaspase3-F	ATGGAGAACAACAAAACCTCAGT
mCaspase3-R	TTGCTCCCATGTATGGTCTTTAC
mCaspase9-F	TCCTGGTACATCGAGACCTTG
mCaspase9-R	AAGTCCCTTTCGCAGAAACAG
mSOD2-F	CAGACCTGCCTTACGACTATGG
mSOD2-R	CTCGGTGGCGTTGAGATTGTT
mSIRT3-F	ATCCCGGACTTCAGATCCCC
mSIRT3-R	CAACATGAAAAAGGGCTTGGG
mPGC1a-F	TATGGAGTGACATAGAGTGTGCT
mPGC1a-R	CCACTTCAATCCACCCAGAAAG
mTFAM-F	ATTCCGAAGTGTTTTTCCAGCA
mTFAM-R	TCTGAAAGTTTTGCATCTGGGT

Table 1. Primer sepuences. F, forward; R, reverse.

Cell viability assay
Approximately 4 × 104 cells were cultured in a 96-well plate. After 24 h incubation, the cells were designated into four groups, as mentioned above, and cultured for 48 h. CCK-8 working solution (Solarbio, China) was added to the cell culture medium and kept for 2 h at 37 °C. To evaluate cell viability, the absorbance (OD) was quantified at 450 nm *via* a microplate reader (Thermo, USA).

Apoptosis analysis
Cellular apoptosis was monitored *via* FC analysis using Annexin V-FITC/propidium iodide (PI) dual staining assay as per the Annexin V-FITC Apoptosis Detection Kit's guidelines (Beyotime, China). KGN cells (4×10^5 cells/well) were allowed to grow into 6-well plates for overnight attachment. After treatment, cells were collected and stained with FITC Annexin V and PI for 15 min at 25 °C, using the Annexin V-FITC Apoptosis Detection Kit. All stained cells were examined *via* FC (BD, USA).

Detection of ROS
The ROS levels within cells were detected in line with the guidelines of the ROS Assay Kit with DCFH-DA (Beyotime, China). KGN cells (4 × 105 cells/well) cultured in 6-well plates or confocal dishes were treated for 48 h. Cells in the confocal plates were stained with DCFH-DA solution for 20 min and then examined via a confocal laser microscope. Cells in 6-well plates were stained with DCFH-DA and analyzed by FCM.

MMP assay
Based on the manufacturer's procedure, this assay was performed using a JC-1 MMP kit (Beyotime, China). KGN cells (4 × 105 cells/well) in 6-well plates or confocal dishes were treated for 48. Cells in the confocal dishes were stained for 20 min with JC-1 solution and visualized via a confocal laser microscope. However, FC analyzed cells within the 6-well plates after harvesting and stained with JC-1.

Real-time PCR analysis
The total content of KGN cells or ovarian tissue using the MiniBEST Universal RNA Extraction Kit (Takara, Japan). Next, cDNA was synthesized *via* the PrimeScript RT reagent Kit (Takara, Japan). Gene expression was measured by PCR analysis on a Real-Time PCR system (Bio-Rad, USA) *via* TB Green Premix Ex TaqII (Takara, Japan). Samples were normalized with *GAPDH*. For the relative quantification of gene expression, the 2-ΔΔCt method was used. Details of primer sequences are depicted in Table 1.

Statistical analysis
Data was statistically examined *via* GraphPad Prism 8 (USA). The data that adhered to the normal distribution were presented as mean ± SEM. The t-test was employed to analyze the variances between the 2 groups, while the one-way analysis of variance (ANOVA) was used to evaluate the variations when more than 2 groups. The level of statistical significance was indicated as * $p < 0.05$, ** $p < 0.01$, and *** $p < 0.001$.

Data availability
All data of this study are available from the corresponding author upon request.

Received: 18 November 2024; Accepted: 17 February 2025
Published online: 10 March 2025

References

1. Lambrinoudaki, I. et al. Premature ovarian insufficiency: a toolkit for the primary care physician. *Maturitas* **147**, 53–63. https://doi.org/10.1016/j.maturitas.2020.11.004 (2021).
2. Ding, X. et al. Potential therapeutic options for premature ovarian insufficiency: experimental and clinical evidence. *Reproductive Sci. (Thousand Oaks Calif)* **30**, 3428–3442. https://doi.org/10.1007/s43032-023-01300-1 (2023).
3. van Dorp, W. et al. Reproductive function and outcomes in Female Survivors of Childhood, adolescent, and Young Adult Cancer: a review. *J. Clin. Oncology: Official J. Am. Soc. Clin. Oncol.* **36**, 2169–2180. https://doi.org/10.1200/jco.2017.76.3441 (2018).
4. Kalich-Philosoph, L. et al. Cyclophosphamide triggers follicle activation and burnout; AS101 prevents follicle loss and preserves fertility. *Sci. Transl. Med.* **5**, 185ra162. https://doi.org/10.1126/scitranslmed.3005402 (2013).
5. Yin, N. et al. Protective properties of heme oxygenase-1 expressed in umbilical cord mesenchymal stem cells help restore the ovarian function of premature ovarian failure mice through activating the JNK/Bcl-2 signal pathway-regulated autophagy and upregulating the circulating of CD8(+)CD28(-) T cells. *Stem Cell Res. Ther.* **11**, 49. https://doi.org/10.1186/s13287-019-1537-x (2020).
6. Yang, M. et al. Bone marrow mesenchymal stem cell-derived exosomal mir-144-5p improves rat ovarian function after chemotherapy-induced ovarian failure by targeting PTEN. *Lab. Invest.* **100**, 342–352. https://doi.org/10.1038/s41374-019-0321-y (2020).
7. Abreu, S. C., Weiss, D. J. & Rocco, P. R. Extracellular vesicles derived from mesenchymal stromal cells: a therapeutic option in respiratory diseases? *Stem Cell Res. Ther.* **7**. https://doi.org/10.1186/s13287-016-0317-0 (2016).
8. Qiu, G. et al. Mesenchymal stem cell-derived extracellular vesicles affect disease outcomes via transfer of microRNAs. *Stem Cell Res. Ther.* **9**. https://doi.org/10.1186/s13287-018-1069-9 (2018).
9. Meldolesi, J. Exosomes and ectosomes in Intercellular Communication. *Curr. Biology: CB*. **28**, R435–r444. https://doi.org/10.1016/j.cub.2018.01.059 (2018).
10. Pluchino, S. & Smith, J. A. Explicating exosomes: reclassifying the Rising Stars of Intercellular Communication. *Cell* **177**, 225–227. https://doi.org/10.1016/j.cell.2019.03.020 (2019).
11. Li, Z. et al. Human umbilical cord mesenchymal stem cell-derived exosomes improve ovarian function and proliferation of premature ovarian insufficiency by regulating the Hippo Signaling Pathway. *Front. Endocrinol.* **12**, 711902. https://doi.org/10.3389/fendo.2021.711902 (2021).
12. Monguió-Tortajada, M. et al. Nanosized UCMSC-derived extracellular vesicles but not conditioned medium exclusively inhibit the inflammatory response of stimulated T cells: implications for nanomedicine. *Theranostics* **7**, 270–284. https://doi.org/10.7150/thno.16154 (2017).
13. Yang, Y., Lee, E. H. & Yang, Z. Hypoxia-conditioned mesenchymal stem cells in tissue regeneration application. *Tissue Eng. Part. B Reviews* **28**, 966–977. https://doi.org/10.1089/ten.TEB.2021.0145 (2022).
14. Zhu, L. P. et al. Hypoxia-elicited mesenchymal stem cell-derived exosomes facilitates cardiac repair through miR-125b-mediated prevention of cell death in myocardial infarction. *Theranostics* **8**, 6163–6177. https://doi.org/10.7150/thno.28021 (2018).
15. Liu, W. et al. Hypoxic mesenchymal stem cell-derived exosomes promote bone fracture healing by the transfer of miR-126. *Acta Biomater.* **103**, 196–212. https://doi.org/10.1016/j.actbio.2019.12.020 (2020).
16. Shin, H. S., Lee, S., Kim, Y. M. & Lim, J. Y. Hypoxia-activated adipose mesenchymal stem cells prevents Irradiation-Induced Salivary Hypofunction by enhanced paracrine effect through fibroblast growth factor 10. *Stem Cells (Dayton Ohio)*. **36**, 1020–1032. https://doi.org/10.1002/stem.2818 (2018).
17. Deng, C. et al. Hypoxic mesenchymal stem cell-derived exosomes promote the survival of skin flaps after ischaemia-reperfusion injury via mTOR/ULK1/FUNDC1 pathways. *J. Nanobiotechnol.* **21**. https://doi.org/10.1186/s12951-023-02098-5 (2023).
18. Xiong, Y. et al. Cyclophosphamide promotes the proliferation inhibition of mouse ovarian granulosa cells and premature ovarian failure by activating the lncRNA-Meg3-p53-p66Shc pathway. *Gene* **596**, 1–8. https://doi.org/10.1016/j.gene.2016.10.011 (2017).
19. Qu, Q. et al. Mir-126-3p containing exosomes derived from human umbilical cord mesenchymal stem cells promote angiogenesis and attenuate ovarian granulosa cell apoptosis in a preclinical rat model of premature ovarian failure. *Stem Cell Res. Ther.* **13**, 352. https://doi.org/10.1186/s13287-022-03056-y (2022).
20. Tsai-Turton, M., Luong, B. T., Tan, Y. & Luderer, U. Cyclophosphamide-induced apoptosis in COV434 human granulosa cells involves oxidative stress and glutathione depletion. *Toxicol. Sci.* **98**, 216–230. https://doi.org/10.1093/toxsci/kfm087 (2007).
21. Męczekalski, B., Maciejewska-Jeske, M. & Podfigurna, A. Reproduction in premature ovarian insufficiency patients - from latest studies to therapeutic approach. *Przeglad Menopauzalny = Menopause Rev.* **17**, 117–119. https://doi.org/10.5114/pm.2018.78554 (2018).
22. Na, J. & Kim, G. J. Recent trends in stem cell therapy for premature ovarian insufficiency and its therapeutic potential: a review. *J. Ovarian Res.* **13**. https://doi.org/10.1186/s13048-020-00671-2 (2020).
23. Ghahremani-Nasab, M., Ghanbari, E., Jahanbani, Y., Mehdizadeh, A. & Yousefi, M. Premature ovarian failure and tissue engineering. *J. Cell. Physiol.* **235**, 4217–4226. https://doi.org/10.1002/jcp.29376 (2020).
24. Sadeghi, S., Mosaffa, N., Huang, B. & Ramezani Tehrani, F. Protective role of stem cells in POI: current status and mechanism of action, a review article. *Heliyon* **10**, e23271. https://doi.org/10.1016/j.heliyon.2023.e23271 (2024).
25. Rahyussalim, A. J., Saleh, I., Kurniawati, T. & Lutfi, A. Improvement of renal function after human umbilical cord mesenchymal stem cell treatment on chronic renal failure and thoracic spinal cord entrapment: a case report. *J. Med. Case Rep.* **11**, 334. https://doi.org/10.1186/s13256-017-1489-7 (2017).
26. Yin, J. Q., Zhu, J. & Ankrum, J. A. Manufacturing of primed mesenchymal stromal cells for therapy. *Nat. Biomedical Eng.* **3**, 90–104. https://doi.org/10.1038/s41551-018-0325-8 (2019).
27. Gowen, A., Shahjin, F., Chand, S., Odegaard, K. E. & Yelamanchili, S. V. Mesenchymal stem cell-derived extracellular vesicles: challenges in clinical applications. *Front. cell. Dev. Biology* **8**, 149. https://doi.org/10.3389/fcell.2020.00149 (2020).
28. Zhu, J. et al. Myocardial reparative functions of exosomes from mesenchymal stem cells are enhanced by hypoxia treatment of the cells via transferring microRNA-210 in an nSMase2-dependent way. *Artif. Cells Nanomed. Biotechnol.* **46**, 1659–1670. https://doi.org/10.1080/21691401.2017.1388249 (2018).
29. Harting, M. T. et al. Inflammation-stimulated mesenchymal stromal cell-derived extracellular vesicles attenuate inflammation. *Stem Cells (Dayton Ohio)* **36**, 79–90. https://doi.org/10.1002/stem.2730 (2018).
30. Zhou, Y. et al. Human mesenchymal stem cells derived exosomes improve ovarian function in chemotherapy-induced premature ovarian insufficiency mice by inhibiting ferroptosis through Nrf2/GPX4 pathway. *J. Ovarian Res.* **17** https://doi.org/10.1186/s13048-024-01403-6 (2024).
31. Yang, Z. et al. Therapeutic effects of human umbilical cord mesenchymal stem cell-derived microvesicles on premature ovarian insufficiency in mice. *Stem Cell Res. Ther.* **10**. https://doi.org/10.1186/s13287-019-1327-5 (2019).
32. May-Panloup, P. et al. Ovarian ageing: the role of mitochondria in oocytes and follicles. *Hum. Reprod. Update.* **22**, 725–743. https://doi.org/10.1093/humupd/dmw028 (2016).
33. Kasapoğlu, I. & Seli, E. Mitochondrial dysfunction and ovarian aging. *Endocrinology* **161**. https://doi.org/10.1210/endocr/bqaa001 (2020).
34. Sytykiewicz, H., Łukasik, I., Goławska, S. & Chrzanowski, G. Aphid-triggered changes in oxidative damage markers of nucleic acids, proteins, and lipids in Maize (Zea mays L.) Seedlings. *Int. J. Mol. Sci.* **20**. https://doi.org/10.3390/ijms20153742 (2019).
35. Lin, L. et al. Reactive oxygen species-induced SIAH1 promotes granulosa cells' senescence in premature ovarian failure. *J. Cell. Mol. Med.* **26**, 2417–2427. https://doi.org/10.1111/jcmm.17264 (2022).

36. Sasaki, H. et al. Impact of oxidative stress on Age-Associated decline in Oocyte Developmental competence. *Front. Endocrinol.* **10**, 811. https://doi.org/10.3389/fendo.2019.00811 (2019).
37. Lv, X. et al. Effects of single and multiple transplantations of human umbilical cord mesenchymal stem cells on the recovery of ovarian function in the treatment of premature ovarian failure in mice. *J. Ovarian Res.* **14**. https://doi.org/10.1186/s13048-021-00871-4 (2021).
38. Théry, C. et al. Minimal information for studies of extracellular vesicles 2018 (MISEV2018): a position statement of the International Society for Extracellular Vesicles and update of the MISEV2014 guidelines. *J. Extracell. Vesicles* **7**, 1535750. https://doi.org/10.1080/20013078.2018.1535750 (2018).
39. Li, Z. et al. Compatibility of Achyranthes bidentata components in reducing inflammatory response through arachidonic acid pathway for treatment of Osteoarthritis. *Bioengineered* **13**, 1746–1757. https://doi.org/10.1080/21655979.2021.2020394 (2022).

Author contributions
Conceptualization, Shanshan Zhang and Yanqun Wu; Formal analysis, Xinfeng Zou; Funding acquisition, Yanqun Wu; Methodology, Xiaona Feng; Project administration, Xiaona Feng, Yanyun Zheng and Qun Li; Resources, Xinfeng Zou and Shuai Shi; Validation, Yanyun Zheng and Qun Li; Writing – original draft, Shanshan Zhang and Yanqun Wu; Writing – review & editing, Shuai Shi and Yanqun Wu.

Funding
This study was supported by the Research Fund for Academician LinHe NewMedicine (JYHL2022MS20), the Key Research and Development Program of Rizhao City (2023ZDYF010144), the Small and Medium Sized Enterprise Innovation Capability Enhancement Project of Shandong Province (2023TSGC0549), the Practical Teaching Education Research Project Plan of Jining Medical University (JYSJ2022B04), Shandong Province medical health science and technology project (202402010756).

Declarations

Competing interests
The authors declare no competing interests.

Ethical approval
Jining Medical University's Animal Care and Use Committee and Augie Medical Ethics Committee of Rizhao City gave ethical approval for the study.

Additional information
Supplementary Information The online version contains supplementary material available at https://doi.org/10.1038/s41598-025-90879-3.

Correspondence and requests for materials should be addressed to Y.W.

Reprints and permissions information is available at www.nature.com/reprints.

Publisher's note Springer Nature remains neutral with regard to jurisdictional claims in published maps and institutional affiliations.